Response of bucket foundations under cyclic loading

Réponse des fondations du seau sous charge cyclique

[Jeong-Seon][Park]
[Civil and Environmental Engineering], [Hanyang University], [Korea], [jpark86@hanyang.ac.kr]

[Duhee][Park]
[Civil and Environmental Engineering], [Hanyang University], [Korea]

ABSTRACT: Estimation of accumulated rotational angles and settlements are critical in design of wind turbine foundation. However, there have been few studies exploring the response of bucket foundation to long-term cyclic loading. We perform a series of three-dimensional finite element analyses of bucket foundations installed in sands. An empirical formulation which captures the stiffness degradation observed in cyclic triaxial tests is implemented into the finite element analysis in the form of a user subroutine.

1 INTRODUCTION

In this study, we performed a series of three-dimensional finite element analyses of bucket foundations installed in sand. An empirical formulation of stiffness degradation of sand is implemented into the analysis using a user subroutine. Using the stiffness degradation model the accumulated rotation and displacement of bucket foundation were calculated. Additionally, important factors affecting the response under cyclic loading were assessed.

2 STIFFNESS DEGRADATION MODEL

The 'stiffness degradation model' is based on an assumption that an increase of the plastic axial strain with the number of cycles in a cyclic triaxial test can be related to the decrease of soil secant stiffness (Figure 1).

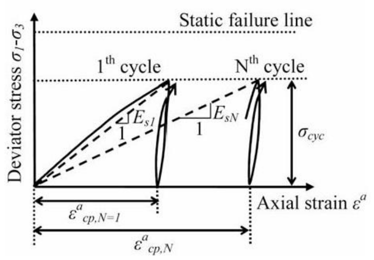

Figure 1. Degradation of soil stiffness during cyclic loading in a drained triaxial test (Achmus et al., 2009)

It is developed by Achmus et al. (2009), and implemented in a finite element analysis to evaluate the long-term performance of monopiles. In Figure 1, if the elastic strain of soil would be negligible, the decreasing rate of secant stiffness after first cycle and *N*th cycle can be presented by the plastic axial strains ratio after first and *N*th cycle according to the following equation:

$$\frac{E_{sN}}{E_{s1}} \simeq \frac{\varepsilon^a_{cp,N=1}}{\varepsilon^a_{cp,N}} \quad (1)$$

where E_{sN} is the secant stiffness of soil, and $\varepsilon^a_{cp,N}$ is the plastic axial strain after *N*th cycle. For cohesionless soils, many empirical equations have been suggested to estimate the accumulated plastic strain in a cyclic triaxial test. Achmus et al. (2009) used the Huurman's formula (Huurman, 1996) which expresses the increase of plastic strain by two empirical parameters and cyclic stress ratio (Eq. (2)).

$$\frac{E_{sN}}{E_{s1}} \simeq \frac{\varepsilon^a_{cp,N=1}}{\varepsilon^a_{cp,N}} = N^{-b_1(X)^{b_2}} \quad (2)$$

where N is the number of load cycles, b_1 and b_2 are empirical coefficients, and X is the cyclic stress ratio defined as follows:

$$X = \frac{\sigma_{1,cyc}}{\sigma_{1,sf}} \quad (3)$$

where $\sigma_{1,sf}$ is the major principal stress at static failure state and $\sigma_{1,cyc}$ is the major principal stress for the cyclic stress state under consideration. The cyclic stress ratio thus is a function of confining stress and applying cyclic load. However, the Eq. (3) is only valid for the triaxial test condition with isotropic initial stress and constant confining pressure. Under the foundation loading conditions, the minor principal stress and the principal stress directions are changed. To solve this problem, a characteristic cyclic stress ratio X_c is defined in his research:

$$X_c = \frac{X^{(1)} - X^{(0)}}{1 - X^{(0)}} \quad (4)$$

where the index $^{(1)}$ is the cyclic stress ratio at loading condition and the index $^{(0)}$ is at unloading phase. The characteristic cyclic stress ratio is determined from the difference between the stress ratios in the loading and the unloading state, and this value varies from 0 to 1. Accumulated plastic strain and the degradation of soil stiffness can be determined from Eq. (2) by replacing X by X_c.

3 FINITE ELEMENT MODEL

The three-dimensional finite element was used to evaluate the long-term response of bucket foundations under cyclic loading (Figure 2). FE analyses were performed using ABAQUS/Standard, and 'stiffness degradation model' was implemented using the user subroutine. Linear elastic-perfectly plastic model following Mohr-Coulomb failure criteria was used to simulate the behavior of sand, and the non-associated flow rule was applied.

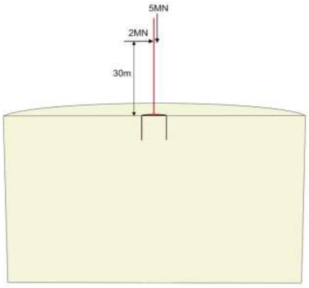

Figure 2. Applying loads on the reference model

The diameter (*D*), length (*L*), and thickness (*t*) of the bucket foundation model were fixed to 10 m, 10 m, and 0.15 m respectively. Two-thirds of the ϕ' of sand was used for the interface friction angle (δ). ϕ' and ψ' of the uniform sand were set to 40° and 10°, and the small cohesion 1 kPa was applied for the stability of the analysis. The unit weight (γ' = 10 kN/m^3), coefficient of lateral earth pressure at rest (K_o = 0.43) and Poisson's ratio (ν = 0.3) of the sand were constant during the analysis, and elastic stiffness (*E*) for the first cycle was set to 35 MPa and changed after *N*th cycles according to the stiffness degradation model. From the documented results of the previous studies, the material constants for dense sand b_1 = 0.2 and b_2 = 5.76 were used in these analyses.

4 NUMERICAL ANALYSIS RESULTS

4.1 *Long-term response of bucket foundations*

The results of accumulated rotations from the calculations are presented in Figure 3. The load was simulated as a loading step from the center to the right direction and an unloading phase in the opposite direction to the left. As the number of repeated loads increase, the magnitude of the cumulative rotational angle of the bucket foundation increases.

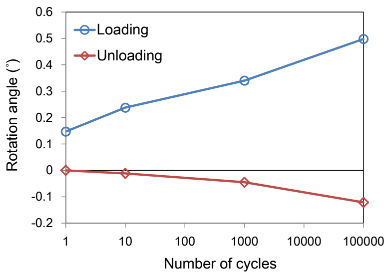

Figure 3. Accumulated deformation of the reference bucket foundation

Figure 4 shows the contours of plastic strain increment after *N*th cyclic loadings. As expected, as the number of cyclic loading increase, the failure area and plastic strain of the surrounding soil increase.

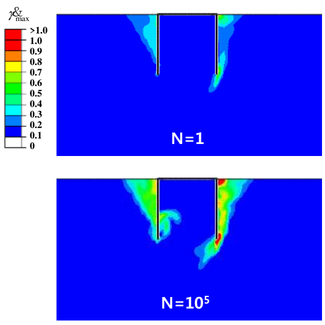

Figure 4. Contour of plastic strain increment after *N*th cyclic loadings

4.2 *Parametric studies*

In order to evaluate the long-term behavior of the bucket foundation according to the external load conditions, the following four load cases were applied (Figure 5)

Figure 6 shows the results of calculating the changes of the rotation angle under cyclic loading in all cases. The results of the reference model are also shown for the comparison. When the acting moment is the same at 60 MN-m and the horizontal load is applied at different positions, the permanent displacement is calculated to be larger as the horizontal load acts at lower height. The difference also increases as the number of cyclic loads increases. The calculated permanent rotations are significantly lower when the moment is 50% (30 MN-m) smaller than these. When the horizontal load is reduced to 1MN compared with 2MN in the reference model, there is a difference of rotation up to 3.6 times. Even when the moment decreases, large deformation occurs when the moment arm length is low. However, the difference is very small than when the moment is larger (60 MN-m).

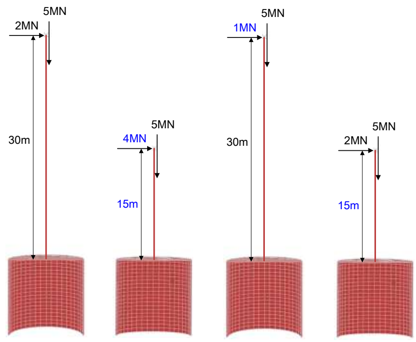

Figure 5. Various loading conditions for the parametric study

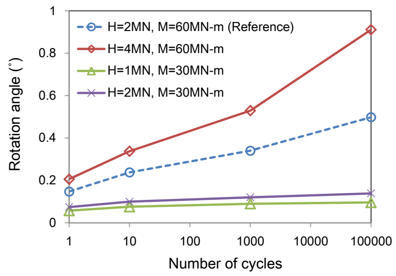

Figure 6. Accumulated deformations from the different horizontal and moment loads

5 CONCLUSIONS

Effects of cyclic loadings are clearly shown to the reference model. As the number of cycles increase, the soil stiffness of the passive and active zones is decreased, and accumulated rotations of the bucket foundation are increased. Due to this, despite one-way loading, permanent deformations occur in the opposite direction when it is unloaded.

6 REFERENCES

Achmus M., Kuo Y.S., and Abdel-Rahman K. 2009. Behavior of monopile foundations under cyclic lateral load. *Computer and Geotechnics* 36 (5), 725-735.

Huurman M. 1996. Development of traffic induced permanent strain in concrete block pavements. *HERON* 41 (4), 29-52.